

# **Petrography in the Rau-1 well, Siri Canyon, Danish North Sea**

Weibel, R., Gjettermann, F. & Friis, H.



# **Petrography in the Rau-1 well, Siri Canyon, Danish North Sea**

Weibel, R., Gjettermann, F. & Friis, H.

Released 30.06.2013

## Summary

Mineralogical quantification is presented for six samples from the Paleogene Ty Member in the Rau-1 well from the Siri Canyon, Danish North Sea. The quantification of detrital grains and authigenic phases is based on point counting of thin sections in transmitted light microscope. Quartz and glauconite are the dominating detrital grains, which furthermore comprise feldspar, mica, skeletal fossils, mudclasts and heavy minerals. The CCSEM (computer controlled scanning electron microscopy) investigations suggest that feldspar grains are more common than given by the point counting results.

Calcite and chlorite are the most important porosity-reducing authigenic phases. Where abundant, calcite completely closes the open porosity. Chlorite on the contrary keeps an internal micro porosity, but has major influence on the permeability. In areas with no (or minor) chlorite and calcite cement the open porosity is up to 13 %. Other authigenic phases include quartz overgrowths, microquartz, pyrite, leucoxene and kaolinite. Scanning electron microscopy of rock chips could verify if microquartz is more abundant.

# Content

<b>Introduction</b>	<b>5</b>
<b>Samples</b>	<b>6</b>
<b>Methods</b>	<b>7</b>
<b>Results and discussion</b>	<b>8</b>
Sediment textures and fabrics .....	8
Detrital grains.....	8
Authigenic phases .....	10
Porosity.....	11
<b>Conclusion</b>	<b>12</b>
<b>References</b>	<b>13</b>
<b>Appendix 1. Point counting results</b>	<b>15</b>
<b>Appendix 2. Thin section overview</b>	<b>17</b>
<b>Appendix 3. Feldspar composition from CCSEM analyses.</b>	<b>27</b>

## **Introduction**

The aim of the investigation is characterisation and quantification of detrital grains, authigenic phases and porosity by point counting thin sections from the Paleogene Ty Member in the Rau-1 well from the Siri Canyon in the Danish North Sea. Additionally, quantification of in particular feldspars is tried by the CCSEM method (computer controlled scanning electron microscopy). This project is initiated by Noreco, Denmark.

## Samples

The thin sections available cover the depth range from 2562.80 m to 2597.75 m. Thin sections with large variation in the degree of cementation are treated as separate samples and are documented by two point countings (a and b in Table 1). All thin sections available at the University of Aarhus have been used, with the exception of one sample that is omitted as it contains only calcite. CCSEM analyses are performed on three samples identical to the thin sections and two additional samples (Tables 1, 2).

**Table 1.** Thin section samples.

Plug/ sample No.	Sample ID	Depth (m)	CCSEM sample at same depth
1	RA1-256280	2562.80	x
2	RA1-256330	2563.30	
4a	RA1-257340	2573.40	x
4b	RA1-257340	2573.40	x
5a	RA1-257420	2574.20	x
5b	RA1-257420	2574.20	x
6	RA1-259575	2595.75	
7a	RA1-259675	2596.75	
7b	RA1-259675	2596.75	

**Table 2.** Samples for CCSEM analyses.

GEUS No.	Sample ID	Depth (m)	Fraction
2003 791	RA1-256280	2562.80	Light fraction
2003 792	RA1-256440	2564.40	Light fraction
2003 793	RA1-257340	2573.40	Light fraction
2003 794	RA1-257340	2573.40	Heavy fraction
2003 795	RA1-259775	2597.75	Light fraction
2003 796	RA1-267420	2674.20	Light fraction
2003 797	RA1-267420	2674.20	Heavy fraction

## Methods

Petrographic investigation of the thin sections was performed by transmitted light microscope. The impregnating epoxy was blue-stained for easier identification of porosity. Quantification took place by point counting a minimum 400 points (grains and porosity) in the thin sections. The texture and mineral group classification, suggested by Noreco, has been applied though with minor adjustments (e.g. division of the feldspar group into K-feldspar and plagioclase).

For the CCSEM method all individual grains needed to be separated in the epoxy in order to be able to identify the minerals, therefore the samples were machine crushed in a tungsten carbide mortar. The crushing was done in several steps, each followed by removal of the fine fraction. The crushing may cause incomplete liberation of the mineral grains, which may appear as artificial rock fragments (e.g. calcite with calcite cement, two individual grains next to each other). The fine fraction was sieved and only the fraction from 45  $\mu\text{m}$  – 1 mm was applied for the CCSEM specimens. Heavy minerals were concentrated by heavy liquid separation using bromoform. The concentrates were embedded in epoxy before grinding and polishing. Polished blocks were carbon coated prior to analysis performed on a Phillips XL 40 scanning electron microscope (SEM) equipped with a Thermo Nanotracer 30  $\text{mm}^2$  detector surface window and a Pioneer Voyager 2.7 10  $\text{mm}^2$  window Si(Li) detector energy dispersive X-ray analysis (EDX) system. The electron beam was generated by a tungsten filament operating at 17 kV and 50-60  $\mu\text{A}$ . The number of measured grains was 1200 in all samples. X-ray data were corrected for atomic number, absorption or fluorescence effects by the Proza correction scheme prior to semi-quantitative, standard-less calculation of elemental concentrations (Bernstein et al. 2008; Keulen et al. 2008). Data reduction was performed on a spreadsheet calculation program developed by GEUS.

# Results and discussion

The thin section petrography is presented in Appendix 1 and transmitted light microscope photos from each sample can be found in Appendix 2. The feldspar composition obtained by CCSEM analyses are shown in Appendix 3.

## Sediment textures and fabrics

The samples studied are mostly very fine-grained to fine-grained sandstones and very well to well sorted (Appendix 1). The maximum quartz grain size varies from coarse-grained to fine-grained. The detrital grains (mainly quartz grains) are generally subangular to sub-rounded. The glauconite grains are typically subrounded, but may be more or less deformed, which is probably due to compaction following the deposition. The grain contacts between quartz grains are typically tangential, indicating that compaction had minor influence on the quartz grains due to the cushioning effect of the glauconite grains.

Most samples appear homogeneous and structureless, though local weak lamination or vague cross stratification may occur.

## Detrital grains

Abundance of grains presented in this section represents mainly results from the point counting of thin sections (Appendix 1). Though, for the feldspar grains results are presented also from the CCSEM method.

### **Monocrystalline quartz (18.5 – 46.3 %)**

Quartz is the most abundant detrital mineral. Monocrystalline quartz grains have dominantly undulating extinctions. The monocrystalline grains are subangular to subrounded.

### **Polycrystalline quartz (3.3 – 11.3 %)**

The polycrystalline grains are typically subrounded.

### **Feldspar (0.8 – 2.8 %)**

The quantification of feldspar by point counting must be taken as a minimum, as the thin sections were not stained for feldspars. Therefore feldspar grains without easy identifiable characteristics, like albite twinning, pericline twinning, perthite exsolution laminae and clearly cleavage, may have been misinterpreted as quartz grains. Results from the CCSEM analyses indicate that K-feldspar seem to be more common (Appendix 3).

CCSEM analyses of similar samples show increased feldspar contents relative to quartz compared with point counting from thin sections (Table 3; Appendix 3).

**Table 3.** Feldspar / quartz and K-feldspar / plagioclase ratios obtained by two methods.

Plug/ sample No.	Sample ID	Depth (m)	K-feldspar / plagioclase ratio		Feldspar / quartz ratio		
			Point counting	CCSEM	Point counting	CCSEM Q85	CCSEM Q75
1	RA1-256280	2562.80	0.12	0.39	0.05	0.19	0.08
2	RA1-256330	2563.30	*		0.04		
-	RA1-266440	2564.40		0.81		0.22	0.08
4a	RA1-257340	2573.40	0.50	0.87	0.05	0.14	0.10
4b	RA1-257340	2573.40	#		0.05		
5a	RA1-257420	2574.20	0.57		0.06		
5b	RA1-257420	2574.20	0.40		0.03		
6	RA1-259575	2595.75	0.50	0.49	0.03	0.15	0.11
7a	RA1-259675	2596.75	0.33		0.04		
7b	RA1-259675	2596.75	0.20		0.03		
-	RA1-267420	2674.20		0.52		0.14	0.10

\* The amount of plagioclase is zero. # The amount of K-feldspar is zero.

Relatively higher amounts of K-feldspar are identified by the CCSEM method, than by point counting. The identification by CCSEM is solely based on the chemical composition of the grains and rock fragments and altered grains may appear with a feldspar-like chemical composition and result in overestimation of the actual amounts of feldspar grains. Furthermore, incomplete liberation of minerals by crushing of the samples may lead to artificial rock fragments, which may not be identified as single minerals and therefore may be underestimated.

The chemical identification criteria of quartz can be chosen to 85 % (Q85: acceptance of up to 15 % of inclusions and intergrowths) or to 75 % (Q75: acceptance of up to 25 % of inclusions and intergrowths). The feldspar / quartz ratio is strongly depending on the chemical definition criteria of quartz by the CCSEM method.

### **Glaucanite (6.3 – 20.3 %)**

Glaucanite pellets or grains are very abundant in all samples. The glaucanite grains appear subrounded, but may also be irregularly shaped due to compaction. Glaucanite pellets, though, may have been underestimated in some samples with high degree of compaction due to incorrect interpretation as chlorite.

### **Mica (1.5 – 4.5 %)**

Mica and glaucanised mica occur in all samples.

### **Glaucanised mica (0.8 – 3.8 %)**

Detrital biotite and chlorite grains are typically partially replaced by glaucanite.

### **Heavy minerals (0.8 – 2.3 %)**

Minerals, such as rutile, apatite, tourmaline, zircon grains, opaque minerals, are accessory. They are typically dominated by opaque grains. Some of the opaque minerals were Fe-Ti oxides, and they are more or less altered to leucoxene. The CCSEM analyses of heavy

minerals concentrates indicate the presence of also garnet, magnetite, monazite, silicate and various mafic silicates (which include amphibole and pyroxene).

#### **Mudstone intraclasts (in one sample 0.3 %)**

Mudstone intraclasts are occasionally found present in the samples.

#### **Skeletal fossils (0 – 0.5 %)**

Rare skeletal fossils are found in most samples.

The detrital composition from point counting suggests that the sandstones are classified as quartzarenites or subarkoses according to Folk (1980). As the sandstones are extremely rich in glauconite the prefix "glaucoparalic" is appropriate. Therefore, the sandstones are glauconitic quartzarenites and (one glauconitic subarkose). The feldspar / quartz ratio obtained by the CCSEM method suggest that the sandstones could be more feldspathic and therefore classified as subarkoses rather than quartzarenites. Verification could be obtained by staining the thin section for feldspar. Unfortunately, there was no time for such procedures in this project.

## **Authigenic phases**

The abundances of the diagenetic phases are from the point counting results (Appendix 1).

#### **Calcite (0 – 48.5 %)**

Calcite occurs in some samples as poikiloplastic cement covering all porosity between the detrital grains or as sporadic cement. The calcite can be distinguished from other carbonates using the chemical composition from the CCSEM analyses. The quantification of calcite by point counting may be overestimated due to its intensive birefringence, which may result in identification of only calcite where it is actually just a thin "wedge". Nevertheless 49 % calcite is a very large amount of cement. It might suggest that the calcite was partly replacing the detrital grains or may have been an early cement that even partly may have been displacive. Calcite-replacement along the rim of detrital grains can be observed.

#### **Chlorite (1.0 – 26.0 %)**

Chlorite is a highly abundant authigenic phase. Its abundance, though, may have been overestimated due to misleading interpretation of squeezed or compressed detrital glauconite grains. In highly porous areas chlorite only fills out minor parts of the pore space. Scanning electron microscopy (SEM) could be a relatively simple way to obtain more information about the nature of the clays.

#### **Quartz (0 – 2.0 %)**

Quartz overgrowths occur in most samples, though in minor amounts. The quartz overgrowths have typically only weakly defined dust rims or non dust rims. Therefore, the quantities of authigenic quartz may have been underestimated in the point counting. Cathodoluminescence, on a scanning electron microscope, is the best way to distinguish between detrital and authigenic quartz in such samples. Quartz overgrowths either formed after the

calcite cement or the identification of minor quartz overgrowths may have been obstructed by the strong birefringence of calcite in intensively calcite-cemented samples.

**Microquartz (one sample 0.3 %)**

Microquartz grains coatings are identified in few samples. However, microquartz grains coatings are very difficult to identify in a transmitted light microscope, whereas investigations by scanning electron microscopy might reveal that it is much more common.

**Kaolinite (0 – 0.8 %)**

Kaolinite occurs in some sample as pore-filling cement.

**Pyrite (trace – 0.5 %)**

Pyrite is a common accessory authigenic phase in most samples. It typically occurs as framboids (with a completely spherical shape).

**Leucoxene (0.2 – 0.8 %)**

Leucoxene is an accessory authigenic phase in most samples. The leucoxene is typically an alteration product of Fe-Ti oxides.

## **Porosity**

Both intragrain and intergrain porosity will typically be underestimated by point counting, as mineral phases smaller or thinner than the thin sections (30 µm) will be taken as solid material. This means that tiny crystal surrounded by epoxy typically will be identified as a mineral phase (especially if it has a distinct colour, as chlorite), despite it in fact only comprise a small part of the pore space. Intragrain porosity is a major issue for glauconite grains as well as most clays. At the boundary between detrital grains and the pores, the mineral phase will typically be more dominating than the pores (even though blue-stained). Consequently, the porosity may be slightly underestimated by point counting the thin sections compared to other porosity measurements. The total macroporosity comprises only a minor amount secondary porosity (i.e. porosity after dissolution of detrital grains or early cement).

## Conclusion

The sandstones are dominantly fine-grained to very fine-grained glauconitic sandstones. Quartz comprises the major part of the detrital grains followed by the glauconite grains, which are also highly abundant. Feldspar grains and micas are less common. Quantification of feldspar grains may have been underestimated due to difficulties with the identification of feldspar as the thin sections were not stained for feldspars.

The CCSEM results indicate that detrital feldspar grains are more common than the point counting suggests. It is recommended to verify the feldspar content by point counting thin sections stained for feldspars.

The major porosity reducing authigenic phases are calcite and chlorite. Calcite completely closes the porosity where it is abundant. On the contrary, the intergranular porosity is connected in samples with high content of chlorite, as microporosity is present in the chlorite cement. Instead the chlorite has a reducing effect on the permeability. The amount of calcite and chlorite may have been overestimated due to the intensive birefringence of calcite and misinterpretation of highly deformed detrital glauconite, respectively. Other authigenic phases comprise quartz overgrowth, leucoxene, pyrite and kaolinite. Microquartz is observed in one sample only. Microquartz has been observed during point counting and as this phase is difficult to identify in transmitted light microscope, its recognition may suggest that its abundance is even higher than given by the point counting results. Further investigations of rock chips by scanning electron microscopy could bring forward more information on the authigenic phases.

## References

Folk, R.L. 1980: Petrology of sedimentary rocks. Hemphill Publishing Company, Austin, Texas, 184p.

Bernstein S., Frei, D., McLimans, R., Knudsen, C. Vasudev, V.N. 2008: Application of CCSEM to heavy mineral deposits: Source of high-Ti ilmenite sand deposits of South Kerala beaches, SW India. *Journal of Geochemical Exploration* **96**, 25–42.

Huggins, F.E., Kosmack, D.A., Huffman, G.P. & Lee, R.J. 1980: Coal mineralogy by SEM analysis. *Scanning Electron Microscopy* **1**, 531–540.

Keulen, N., Frei, D., Bernstein, S., Hutchison, M.T., Knudsen C., & Jensen L. 2008: Fully automated analysis of grain chemistry, size and morphology by CCSEM: examples from cement production and diamond exploration. *Reviews of the Survey's Activities 2007*, Geological Survey of Denmark and Greenland, 93–96.

Knudsen, C., Frei, D. Rasmussen, T. Rasmussen, E. S. & McLimans, R. 2005: New methods in provenance studies based on heavy minerals: an example from Miocene sands in Jylland, Denmark. In: Sønderholm, M. & Higgins, A. K. (Eds.) *Review of Survey activities 2004*. Geological Survey of Denmark and Greenland Bulletin **7**, 29–32.



## **Appendix 1. Point counting results**

The point counting results are presented in the table on the following page.





## **Appendix 2. Thin section overview**

Three representative microscope photos have been taken from each sample in order to give a brief overview (Plate 1 to 9 in the following).

Note that the epoxy is stained blue for easier identification of porosity.

# Plate 1

Well: Rau-1  
Depth: 2562.80 m  
Sample No.: 1  
Formation: Ty  
Lithology: Glauconitic sandstone  
Comments:

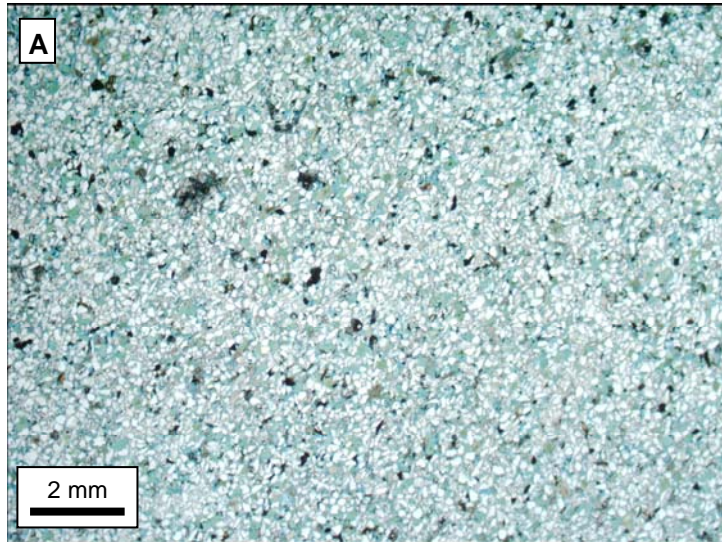


**Fig. A:** Plane polarised light

**Fig. B:** Plane polarised light

**Fig. C:** Crossed polarised light

Figs. A, B and C show that this interval can be described as a very fine-grained glauconitic sandstone.

Figure A shows sporadic patterns of calcite cement.

Figures B and C illustrate that the chlorite content varies and occur both as a pore-filling cement and as clay rims around the detrital grains. The glauconite grains show some degree of deformation due to mechanical compaction. Note that the intergranular porosity is connected, although the chlorite in the pores has a reducing effect on the permeability.

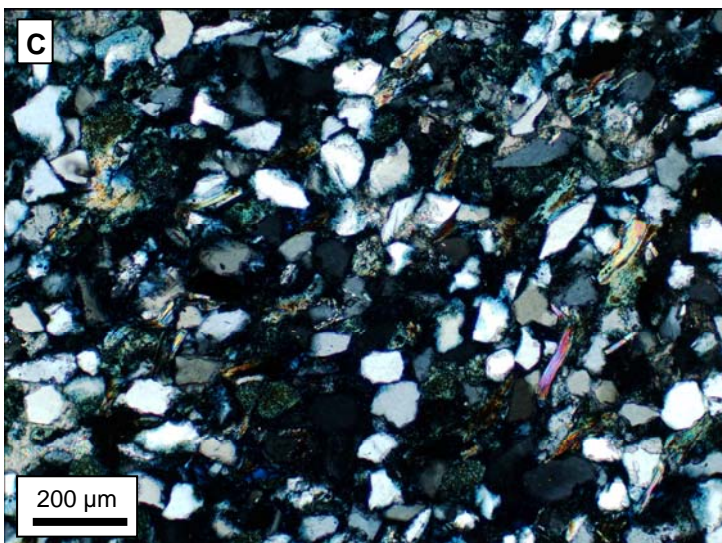
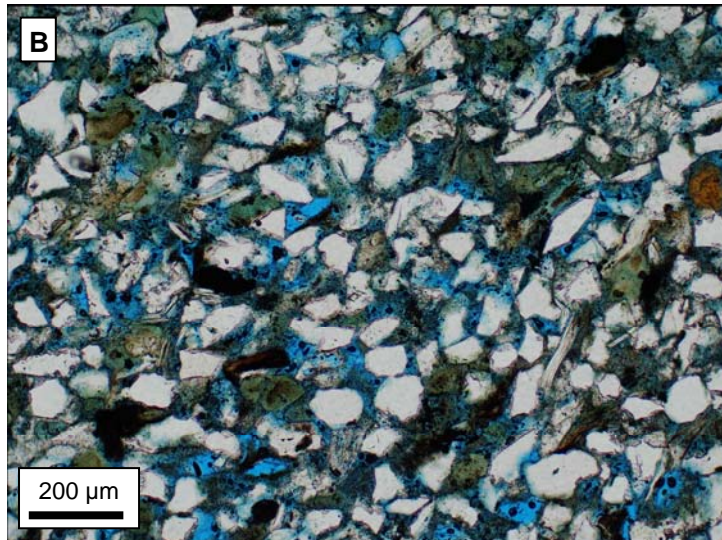


## Plate 2

Well: Rau-1  
Depth: 2563.30 m  
Sample No.: 2  
Formation: Ty  
Lithology: Glauconitic sandstone  
Comments:

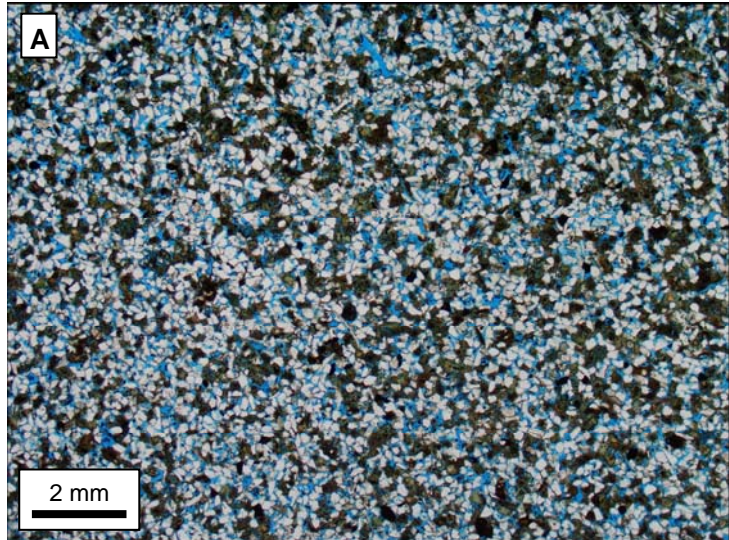


**Fig. A:** Plane polarised light  
**Fig. B:** Plane polarised light  
**Fig. C:** Crossed polarised light

Fig. A shows that this sample is a homogeneous very fine-grained sandstone.

Figs. B and C show that the amount of chlorite content varies and occurs both as a pore-filling cement and as clay rims around detrital grains.

The glauconite grains show some degree of deformation due to mechanical compaction. Note that the intergranular porosity is connected, though the authigenic chlorite has a reducing effect on the permeability.

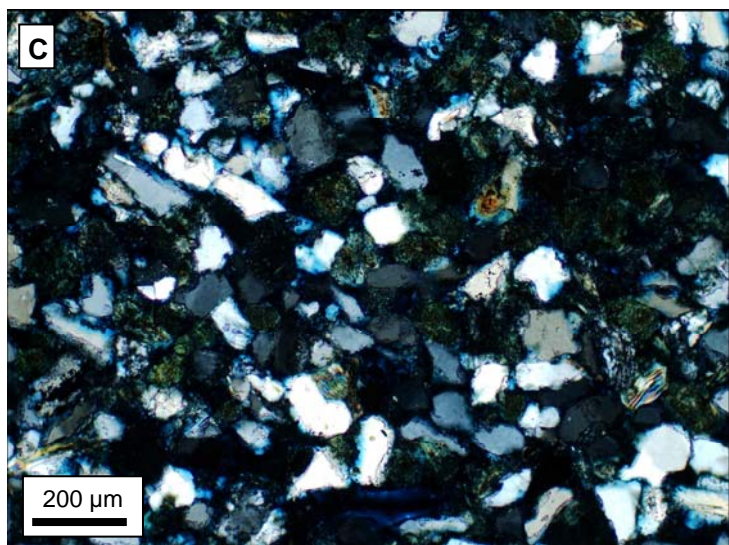
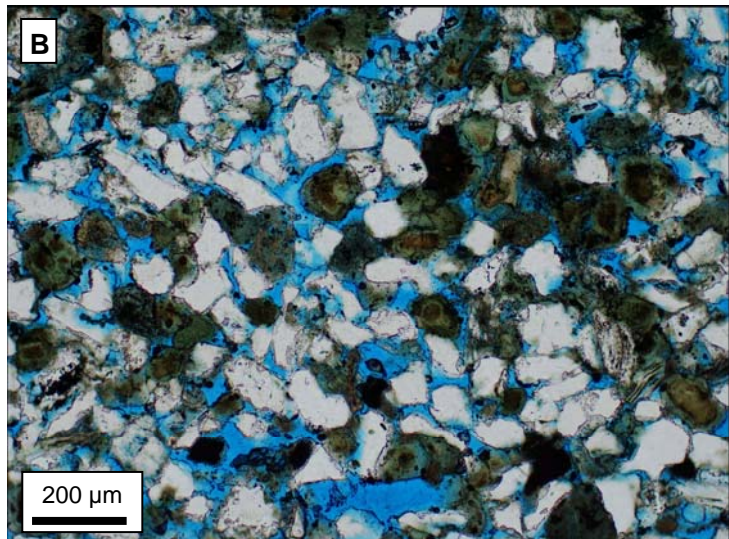


# Plate 3

Well: Rau-1  
Depth: 2573.40 m  
Sample No.: 4a  
Formation: Ty  
Lithology: Glauconitic sandstone  
Comments:

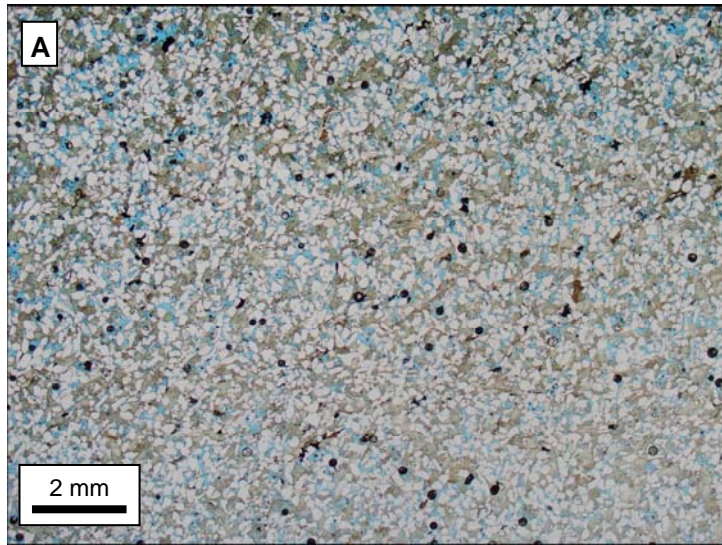


**Fig. A:** Plane polarised light  
**Fig. B:** Plane polarised light  
**Fig. C:** Crossed polarised light

Fig. A shows that this sample is a homogeneous very fine-grained glauconitic sandstone. Fig. B and C show that the chlorite content varies and occur both as a pore-filling cement and as clay rims around detrital grains.

The glauconite grains show some degree of deformation due to mechanical compaction. Note that the intergranular porosity is connected, though the chlorite has a reducing effect on the permeability. Several heavy minerals are found in this samples, and a zircon grain (arrow) can be seen in Figs. B and C.

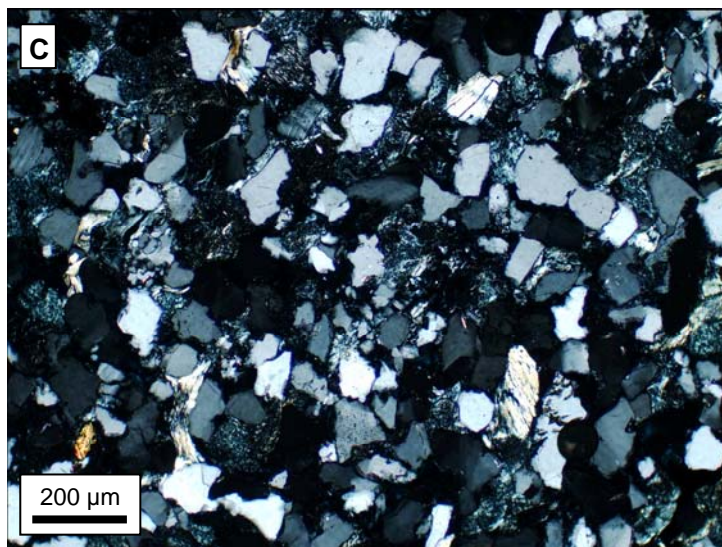
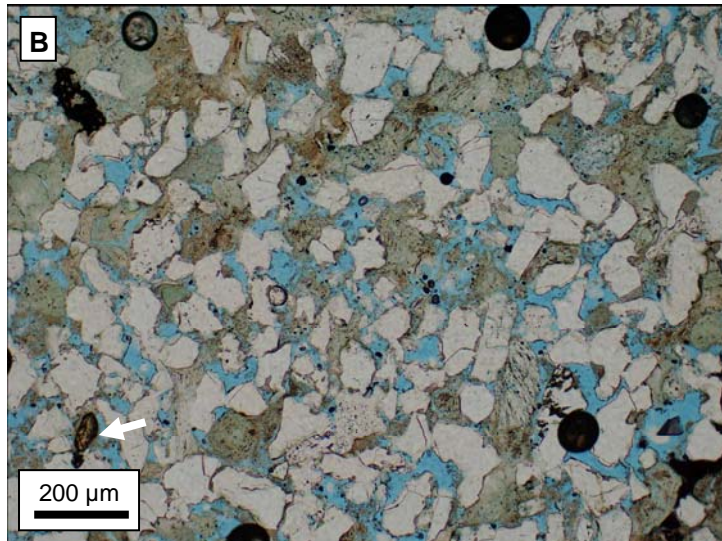


## Plate 4

Well: Rau-1  
Depth: 2573.40 m  
Sample No.: 4b  
Formation: Ty  
Lithology: Calcareous  
glauconitic  
sandstone

Comments:

**Fig. A:** Plane polarised light  
**Fig. B:** Plane polarised light  
**Fig. C:** Crossed polarised light

Figs. A, B and C show that this sample can be described as a very fine-grained calcareous glauconitic sandstone. It is almost completely cemented by poikilotopic calcite. The calcite cement seems to have a corrosive behaviour against some of the detrital grains. The glauconite grains show almost no deformation due to compaction, which indicates that the calcite cementation is an early diagenetic state. Quartz overgrowths are not observed.

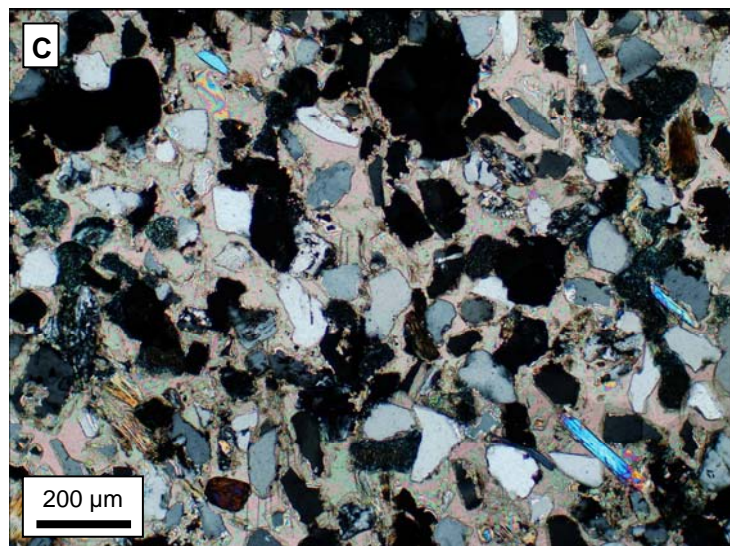
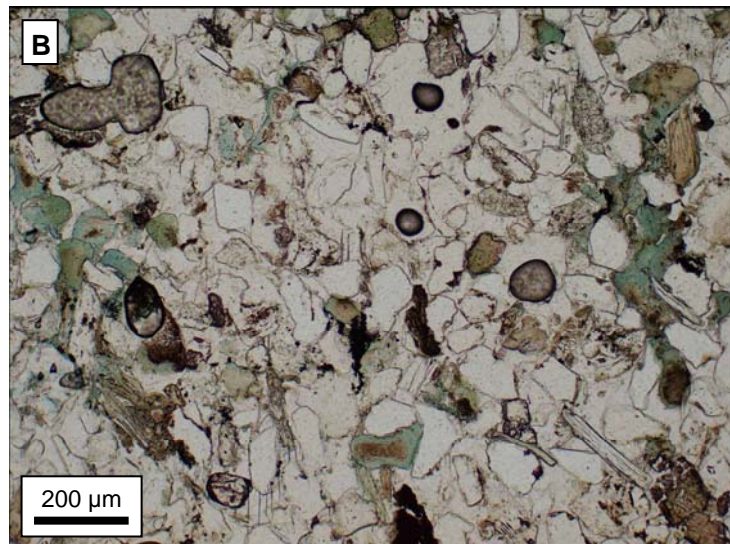
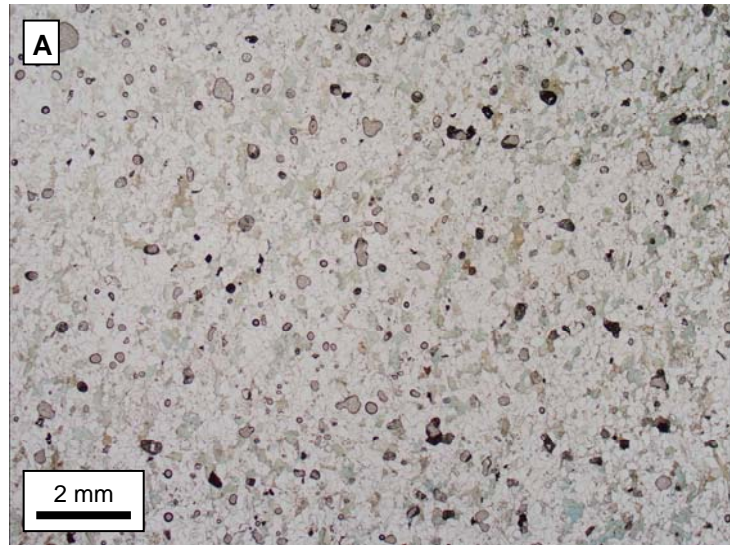


## Plate 5

Well: Rau-1  
Depth: 2574.20 m  
Sample No.: 5a  
Formation: Ty  
Lithology: Glauconitic sandstone  
Comments:

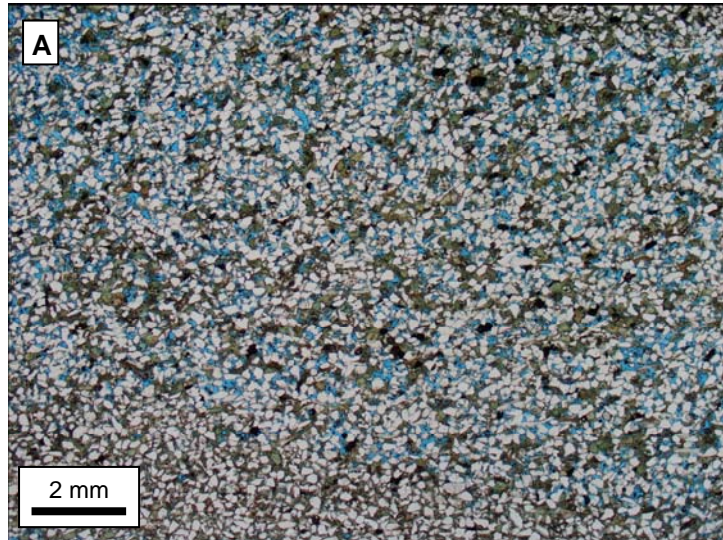


**Fig. A:** Plane polarised light  
**Fig. B:** Plane polarised light  
**Fig. C:** Crossed polarised light

Figs. A, B and C show that this interval can be described as a very fine-grained glauconitic sandstone. The lower part of Fig. A has a lamina almost without porosity but filled with squeezed glauconite grains and/or chlorite. It is difficult to distinguish between the detrital glauconite and authigenic chlorite. Two compacted laminae are observed in this thin section separated by 0,5 mm laminae of higher porosity. The formation of this lamina could be a result of sorting, so laminae with exceptional high amounts with of glauconite grains would more exposed to compaction or they could have been caused by stress zones formed early after deposition. The glauconite grains are generally weakly deformed due to mechanical compaction.

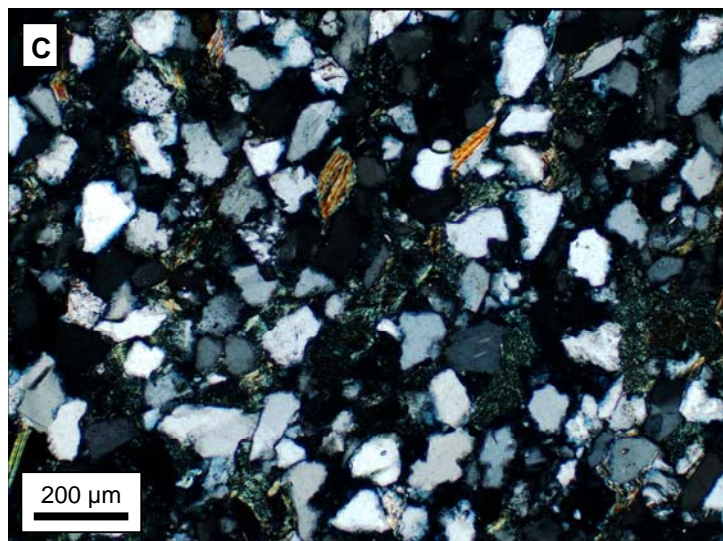
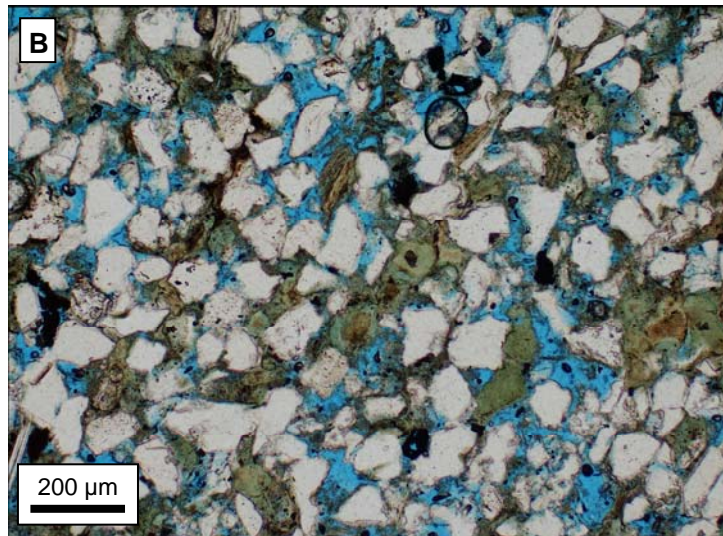


## Plate 6

Well: Rau-1  
Depth: 2574.20 m  
Sample No.: 5b  
Formation: Ty  
Lithology: Glauconitic sandstone  
Comments:

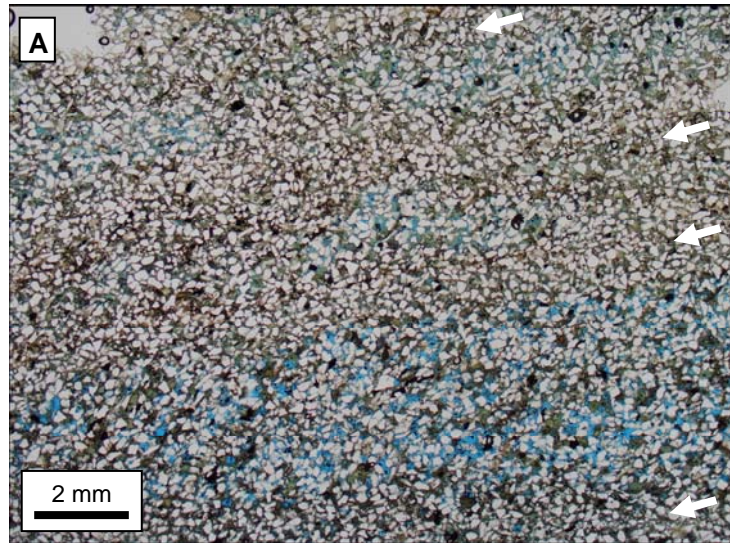


**Fig. A:** Plane polarised light  
**Fig. B:** Plane polarised light  
**Fig. C:** Crossed polarised light

Figures A, B and C show that this interval can be described as a fine-grained glauconitic sandstone. This thin section is very heterogeneous, with zones of high porosity and laminae of deformed glauconite and/or chlorite. It is not possible to distinguish between detrital glauconite and authigenic chlorite. Four laminae are present in this thin section (arrows in Fig. A). These dense laminae could be a result of sorting, so laminae with exceptional high amounts with of glauconite grains would more exposed to compaction or they could have been caused by stress zones formed early after deposition.

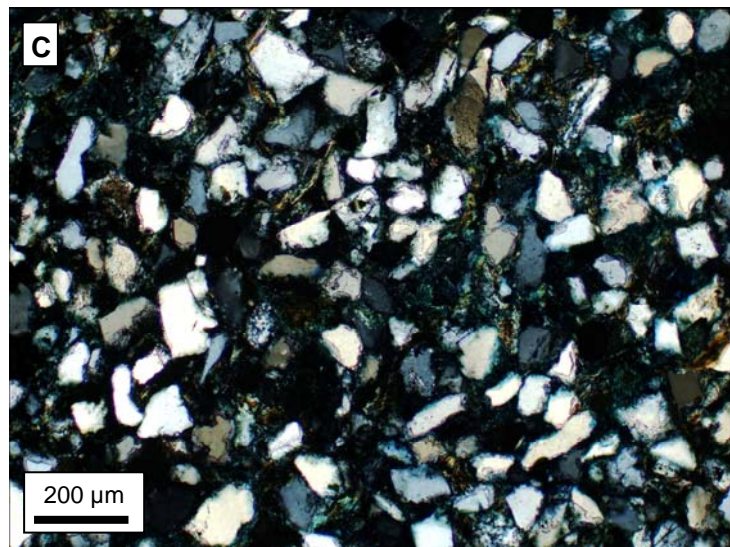
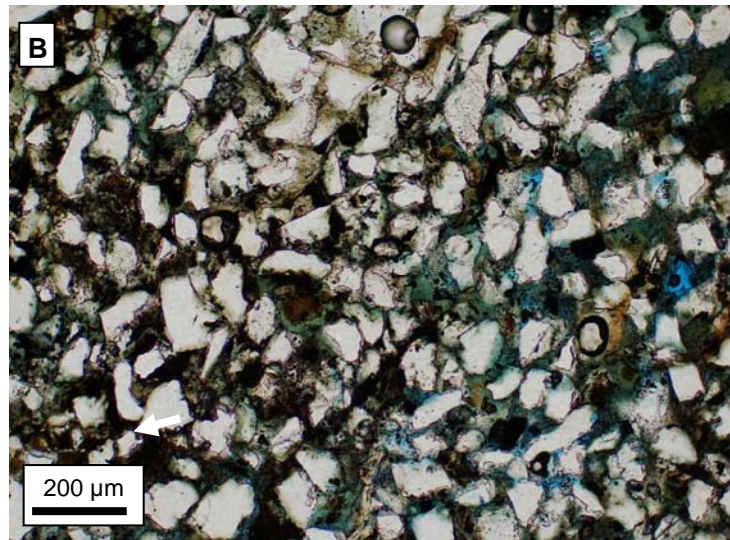


## Plate 7

Well: Rau-1  
Depth: 2595.75 m  
Sample No.: 6  
Formation: Ty  
Lithology: Calcareous  
glaucinitic  
sandstone

Comments:

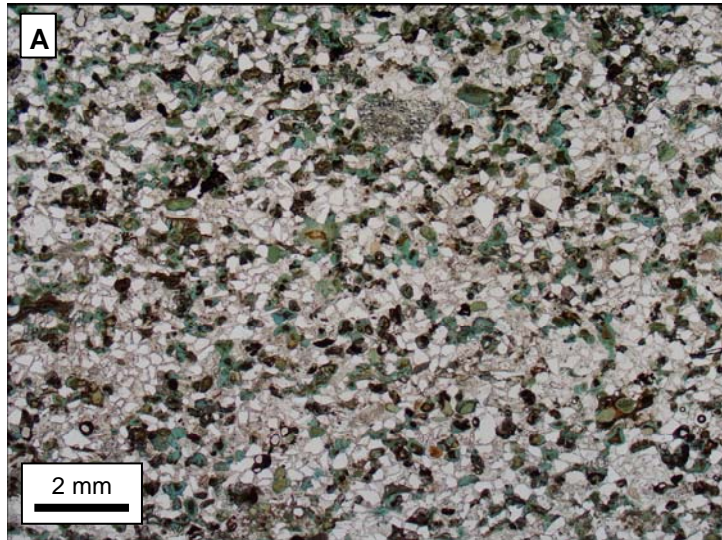


**Fig. A:** Plane polarised light  
**Fig. B:** Plane polarised light  
**Fig. C:** Crossed polarised light

Figures A, B and C show that this interval can be described as a fine-grained glauconitic sandstone almost completely cemented by poikilotopic calcite. The detrital glauconite grains show only weak deformation due to mechanical compaction, which indicates that the calcite cementation is early diagenetic.

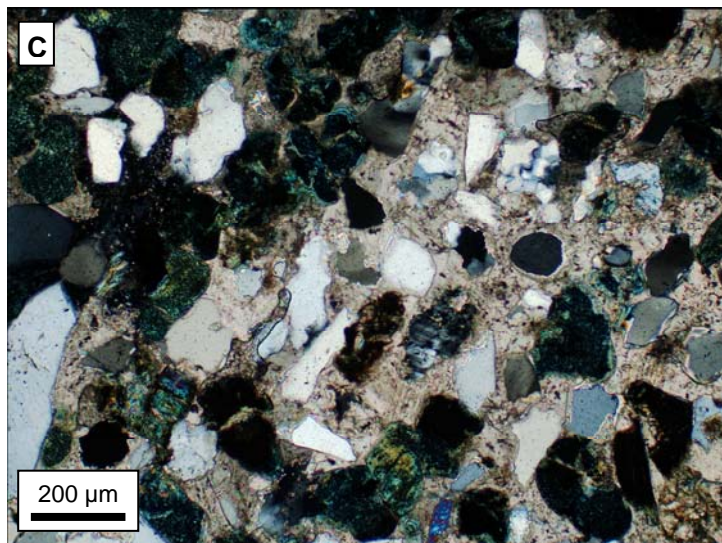
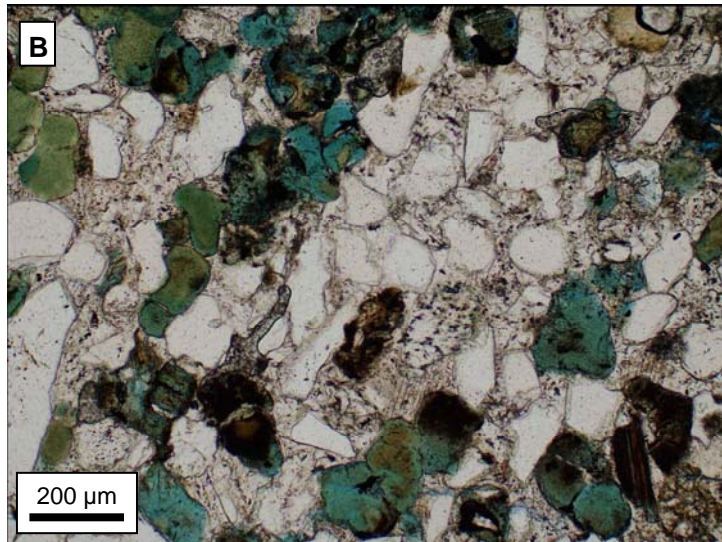


## Plate 8

Well: Rau-1  
Depth: 2596.75 m  
Sample No.: 7a  
Formation: Ty  
Lithology: Glauconitic sandstone  
Comments:

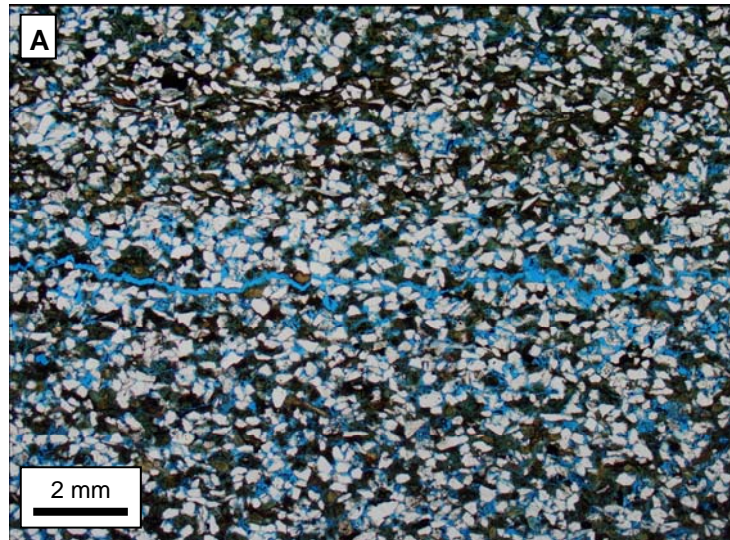


**Fig. A:** Plane polarised light  
**Fig. B:** Plane polarised light  
**Fig. C:** Crossed polarised light

Figs. A, B and C show that this interval can be described as a fine-grained glauconitic sandstone. A zone is observed of almost no porosity in the top of the thin section (Fig. A). Instead it is completely filled with flattened glauconite and/or chlorite. In this zone it is not possible to distinguish between deformed detrital glauconite grains and authigenic chlorite. These dense laminae could be a result of sorting, so laminae with exceptional high amounts with of glauconite grains would more exposed to compaction or they could have been caused by stress zones formed early after deposition. The intergranular porosity is well connected in the porous interval between the more dense laminae (Fig. B).

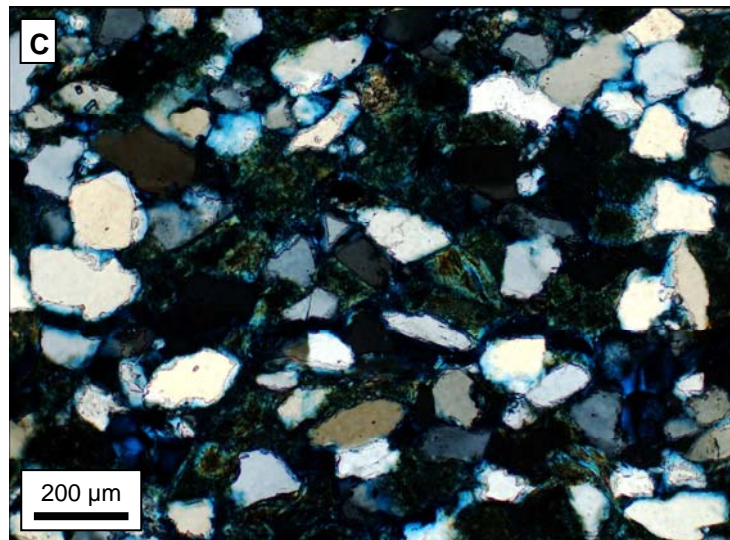
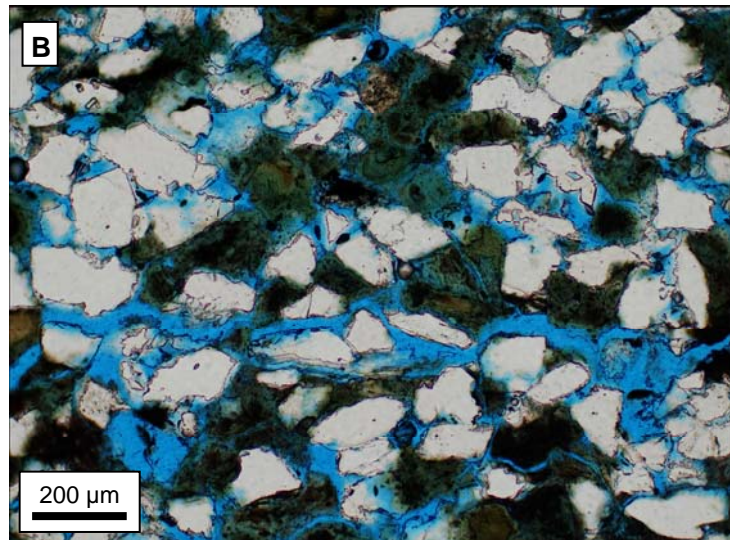


# Plate 9

Well: Rau-1  
Depth: 2597.75 m  
Sample No.: 7b  
Formation: Ty  
Lithology: Glauconitic sandstone  
Comments:

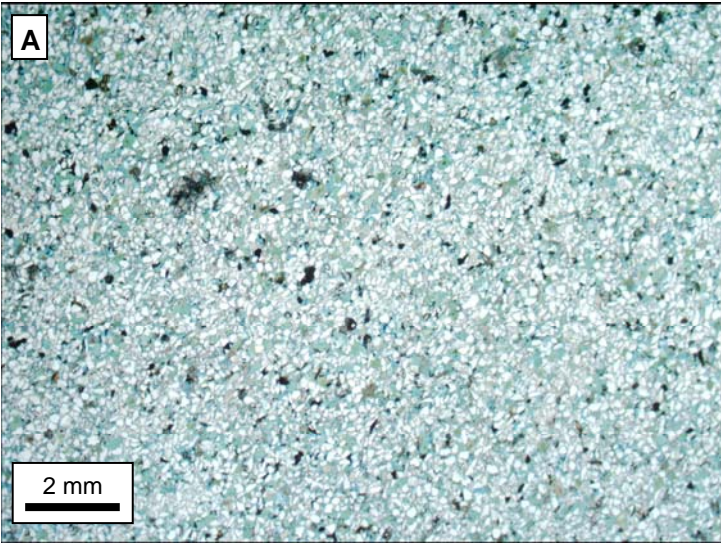
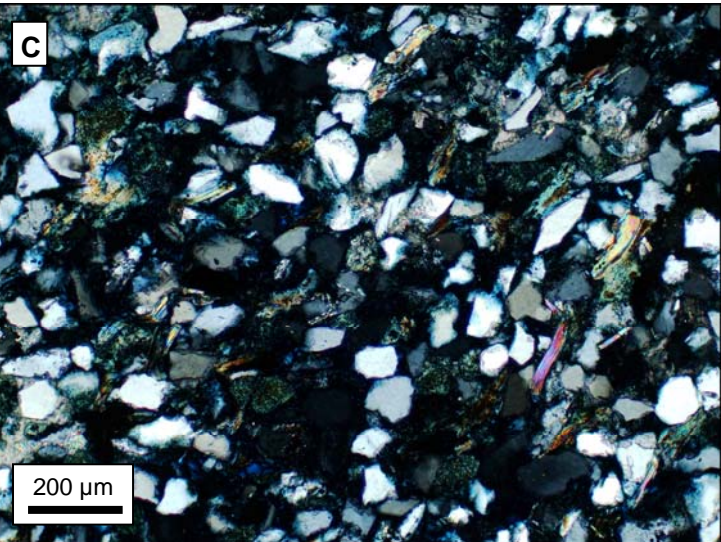
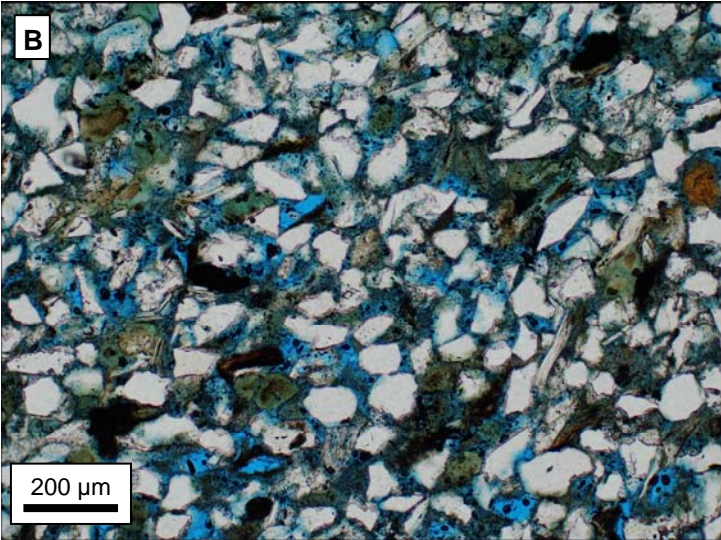


**Fig. A:** Plane polarised light  
**Fig. B:** Plane polarised light  
**Fig. C:** Crossed polarised light

Figures A, B and C show that this interval can be described as a fine-grained glauconitic sandstone. The sample is heterogeneous and contains zones completely cemented with poikilotopic calcite cement, zones partially calcite cemented and other zones without calcite cement. Zones without calcite cement have well connected porosity. The glauconite grains show only weak deformation due to compaction, which could indicate that the calcite cement formed early diagenetic.



### Appendix 3. Feldspar composition from CCSEM analyses.

The CCSEM method was originally developed with purpose of characterisation coal mineralogy (Huggins et al. 1980) and later for identifying heavy minerals in the heavy concentrates of all kind of rock samples (e.g. Knudsen et al. 2005; Bernstein et al. 2008). The method, though, is under constant development and here it has also been applied on the light fraction of sandstones. A complete quantification of all minerals in the samples is the final goal.

All individual grains need to be separated in the epoxy in order to be able to identify the minerals by the CCSEM method, therefore the samples are crushed. The crushing may cause incomplete liberation of the mineral grains. The present method of crushing the samples will have a disproportionate impact on the fragile grains, such as glauconite, which will be lost during sample preparation. Furthermore, the major interest was the distribution of the feldspars, as this information was expected to be difficult to achieve from the thin sections, as they were not stained for feldspars. Consequently, the results are reported for the quartz and feldspar grains only.

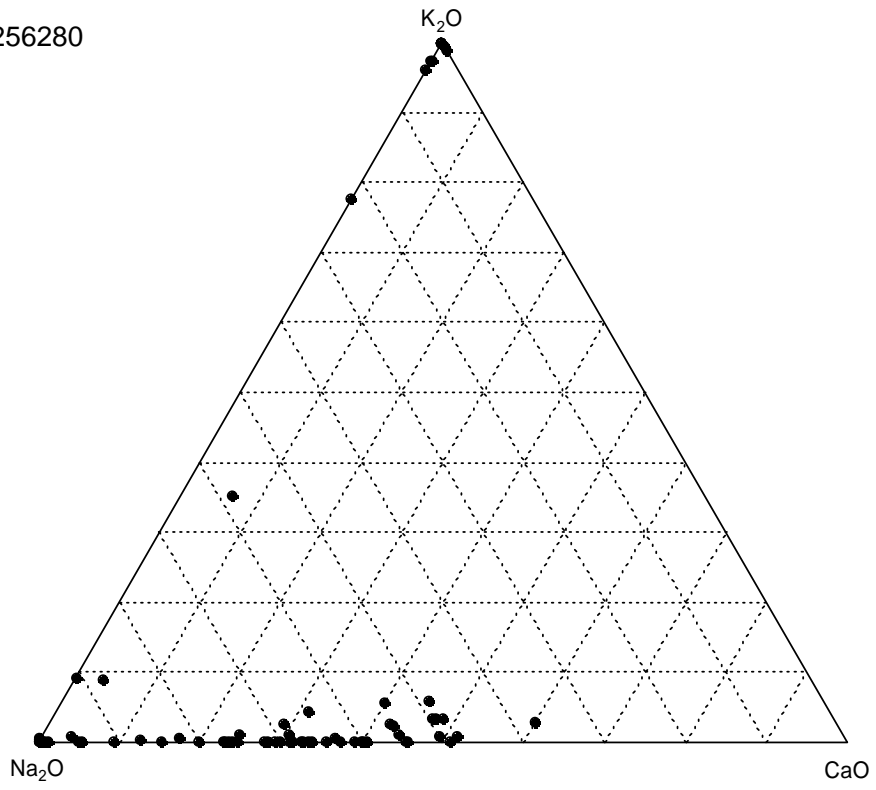
The chemical composition is applied for mineral identification by the CCSEM method. In this study the feldspar grains were identified by the following:

SiO<sub>2</sub>: 40 – 70 wt%  
Al<sub>2</sub>O<sub>3</sub>: 15 – 30 wt (K-feldspar: 15 – 25 wt%)  
K<sub>2</sub>O: 11 – 18 wt% or Na<sub>2</sub>O: 0 – 12 wt% or CaO: 0 – 19 wt%  
Fe<sub>2</sub>O<sub>3</sub>: < 3 wt%  
MgO: < 1 wt%

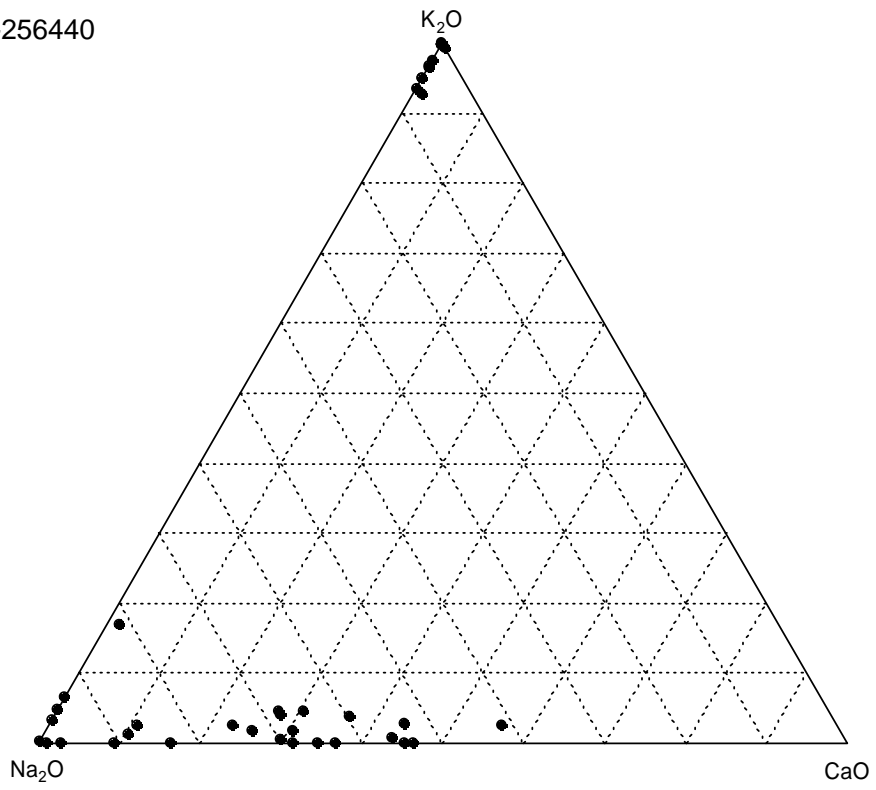
Quartz grains should theoretically have 100 wt% SiO<sub>2</sub>, however inclusions and intergrowth may be part of the grains. Also the sample preparation by crushing may lead to incomplete liberation of the minerals grains (e.g. quartz with some calcite cement, two grains placed next to each other). Therefore a high (up to 15 – 25 wt%) amount of impurities, due to the possible influence from inclusions, intergrowths or neighbouring grains must be accepted.

Ternary plots showing the distribution of the feldspars grains in the investigated samples are presented in the following.

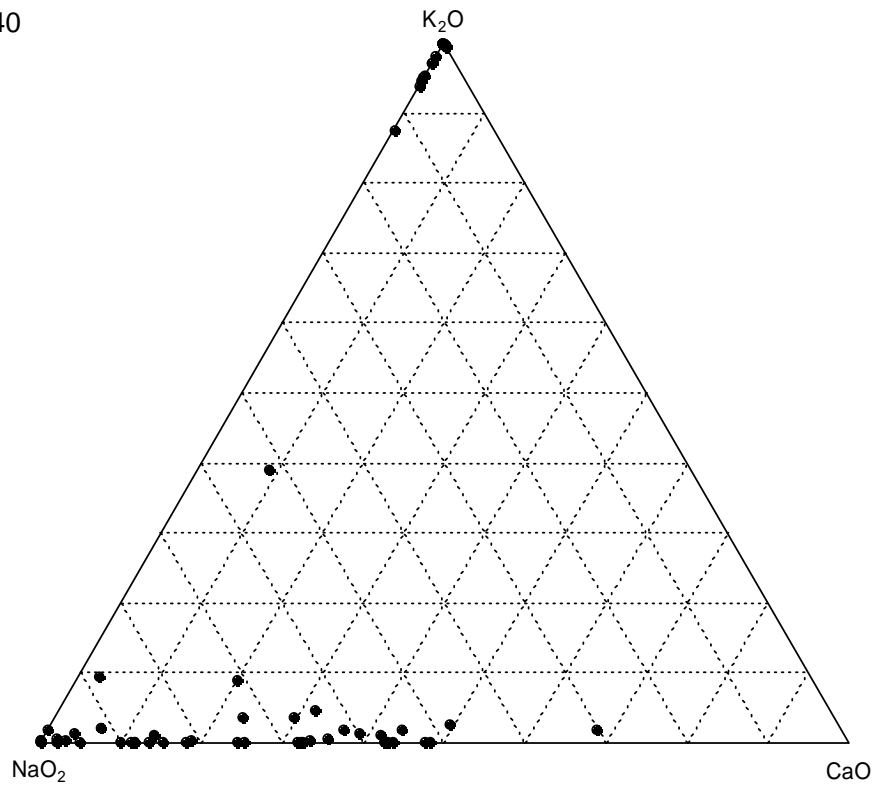
RA1-256280



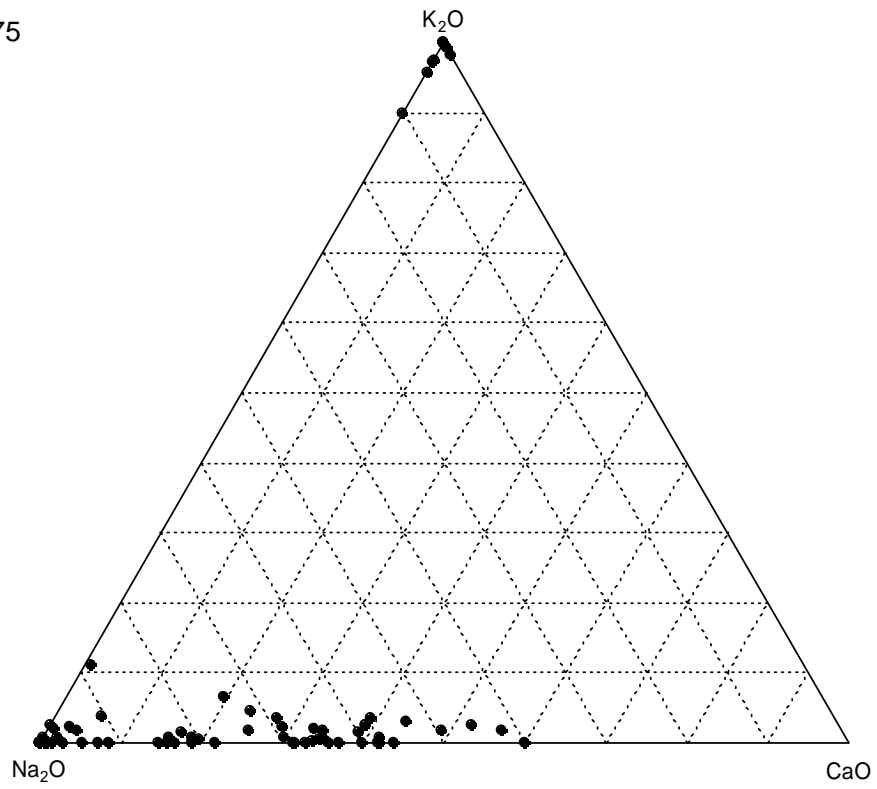
RA1-256440



RA1-257340



RA1-259775



RA1-267420

